



HAL
open science

Composition dependent performance of alumina-based oxide supported WO₃ catalysts for the NH₃-SCR reaction and the NSR plus SCR coupled process

Fabien Can, Xavier Courtois, Sebastien Berland, Mickael Seneque, Sebastien Royer, Daniel Duprez

► To cite this version:

Fabien Can, Xavier Courtois, Sebastien Berland, Mickael Seneque, Sebastien Royer, et al.. Composition dependent performance of alumina-based oxide supported WO₃ catalysts for the NH₃-SCR reaction and the NSR plus SCR coupled process. *Catalysis Today*, 2015, 257, pp.41-50. 10.1016/j.cattod.2015.03.024 . hal-01330404

HAL Id: hal-01330404

<https://hal.science/hal-01330404>

Submitted on 22 Jan 2021

HAL is a multi-disciplinary open access archive for the deposit and dissemination of scientific research documents, whether they are published or not. The documents may come from teaching and research institutions in France or abroad, or from public or private research centers.

L'archive ouverte pluridisciplinaire **HAL**, est destinée au dépôt et à la diffusion de documents scientifiques de niveau recherche, publiés ou non, émanant des établissements d'enseignement et de recherche français ou étrangers, des laboratoires publics ou privés.

Composition dependent performance of alumina-based oxide supported WO₃ catalysts for the NH₃-SCR reaction and the NSR+SCR coupled process.

Fabien Can*, Xavier Courtois, Sébastien Berland, Mickael Seneque, Sébastien Royer, Daniel Duprez

Université de Poitiers, CNRS UMR 7285, IC2MP, 4 Rue Michel Brunet, TSA 51106, 86073 Poitiers Cedex 9, France.

Phone: +33 549453997; mail: fabien.can@univ-poitiers.fr

Abstract

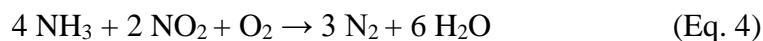
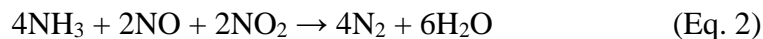
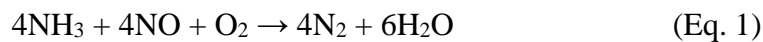
Among the specific technologies to reduce NO_x from automobile lean exhaust gases, the NO_x storage reduction (NSR) and the selective catalytic reduction (SCR) by urea/NH₃ are the two main effective proposed processes. During the short rich excursions of the NSR process, emissions of undesired NH₃ can occur and the combination of the NSR and a NH₃-SCR catalyst has been proposed to improve the global treatment efficiency. With the aim to develop non zeolite SCR catalysts, materials based on modified alumina were prepared by sol-gel method. Necessary acidic and redox properties were expected by incorporation of metal ions such as cerium (for oxygen mobility), zirconium, titanium, and silica (acidic behavior). The influence of each element incorporated in the host alumina and their combination were evaluated in NH₃-SCR before and after 9_{wt}% WO₃ impregnation. Among the 15 synthesized supports, three WO₃ supported catalysts exhibited promising SCR activities were selected (WO₃/Al_{0.2}Ce_{0.4}Ti_{0.4}, WO₃/Al_{0.2}Ce_{0.16}Zr_{0.32}Ti_{0.32} and WO₃/Al_{0.1}Si_{0.1}Ce_{0.16}Zr_{0.32}Ti_{0.32}) and characterized (N₂ adsorption, XRD analysis, NH₃-SCO reactivity, NH₃ storage capacity, pyridine adsorption monitored by IR spectroscopy, H₂-TPR, OSC) and then associated downstream to a model Pt/Ba/Al₂O₃ NSR catalyst. The use of ammonia emitted from the NSR catalyst during the rich pulses was studied taking into accounts three possibilities: the NH₃-SCR reaction (NH₃+NO_x→N₂), the NH₃-SCO reaction (NH₃+O₂→N₂) and the unconverted NH₃. Only the NH₃-SCR reaction occurs at 200°C; whereas the three pathways take place at 300 and 400°C. In addition, a lack of strong acidic storage sites results in unconverted ammonia at high temperature.

Keyword: NH₃; SCR; NSR; LNT; WO₃; alumina.

INTRODUCTION

In order to reduce CO₂ emissions, direct-injection lean-burn engines are attractive for car manufacturers due to the lower fuel consumption. However, these engines operate with a large air excess, which makes very difficult the NO_x abatement in the post treatment catalytic converters. One possible way to reduce NO_x emissions in excess of oxygen is the use of a NO_x storage reduction (NSR) catalyst [1]. It works mainly in lean condition. NO_x are firstly oxidized on precious metals and then stored on basic compounds, mainly as nitrates. Periodically, the catalyst is submitted to rich conditions for few seconds, so that the stored NO_x are reduced into N₂ on the precious metals. Unfortunately, the process can be not fully selective into N₂. In fact, depending on the nature and the concentration of the reductant agent, and the duration of the rich excursion, both N₂O and NH₃ can be observed during the NO_x reduction [2-8]. For instance, it is reported that N₂O yields is enhanced by C₃H₆ at 300°C, whereas NH₃ emission is mainly observed when H₂ is used as reductant [9,10].

To the opposite, SCR is a continuous process. It remains described as an attractive way to reduce NO_x in excess of O₂, with the use of a large choice of reductants like hydrocarbons (HC) [11-19], ammonia [20-23], urea [24], hydrogen [25], alcohol [26,27], *etc.* While HC-SCR was largely studied in the past decades, the NH₃-SCR is accepted to exhibit the highest potential to reduce NO_x emission from Diesel engines. Ammonia reacts with NO_x, according to NH₃-SCR reaction pathways described by Eqs 1 to 4. These reactions are usually denoted as “standard” (Eq. 1), “fast” (Eq. 2), “NO₂-SCR” (Eq. 3, 4) reactions [20,28-32]:



NH₃-SCR catalysts were initially developed for stationary source implementation, for nitric acid production units for instance. V₂O₅-WO₃/TiO₂ catalysts are usually selected for this application [33,34]. These kinds of formulations are also used since 2003 for heavy duty vehicles exhaust gas treatment to reach Euro IV regulation. The thermal stability of these catalysts can be improved by the introduction of rare earth elements. Casanova *et al.* reported that rare earth addition into a V₂O₅/TiO₂-WO₃-SiO₂ limits of the transformation of the TiO₂ anatase phase (high surface area) into rutile (low surface area) [35,36]. ZrO₂ addition to V₂O₅-WO₃/TiO₂ was also reported to inhibit the shrinking of catalyst surface area and the growth of the TiO₂ crystallites [37]. However, vanadium oxide is not suitable for high temperature application because it may sublime for temperature higher than 650°C [38,39].

As a consequence, $V_2O_5-WO_3/TiO_2$ catalysts are not supposed to be associated with a diesel particulate filter (DPF) or a NSR catalyst which can generate high temperature peaks during the regenerations. Up to date, important efforts focus on the development of new low-temperature SCR vanadium-free catalysts, with good activity, high selectivity and high thermal stability. Researches essentially deal on metal-exchanged zeolites [40-47], or oxide-based materials [48]. Zeolite with narrow pores, such as MOR, FER, BEA, and ZSM-5 appeared suitable for SCR applications when exchanged by Fe or Cu. However, it is reported that metal-exchanged zeolite are rather sensitive to the NO_2/NO_x ratio [49-,52].

Then, efforts are made to propose supported transition metal catalysts, such as $Fe_2O_3/WO_3/ZrO_2$ [53] or MnO_x-CeO_2 [54], which are reported to be active in standard conditions (Eq. 1). Indeed, the main elements reported in literature for NH_3 -SCR catalysts are commonly W, Ce, Ti, Si.

WO_3 was reported to enhance the SCR activity of CeO_2/TiO_2 catalysts [55] due to interaction between Ce and W, leading to (i) high dispersion of CeO_2 and WO_3 and to (ii) Ce^{+3} species formation. More recently, Shan *et al.* [56] also reported the high efficiency in NH_3 -SCR of mixed oxides composed of the same elements (W-Ce-Ti). In addition to high CeO_2 and WO_3 dispersion, they suggested that tungsten species enhance the low temperature activity by promoting NO oxidation into NO_2 , thus improving the “fast SCR” reaction (Eq. 2). Small CeO_2 crystallites were also proposed to be responsible of the high NH_3 -SCR activity of cerium-tungsten mixed oxide [57]. Tungsten species was also reported by Chen *et al.* to improve the high temperature N_2 selectivity by supplying large NH_3 adsorption capacity of and inhibiting the NH_3 oxidation into N_2O or NO_x [58].

With the aim to develop non zeolite and thermally stable SCR catalysts able to be associated with a NSR catalyst, vanadium free materials are expected. Catalyst formulation have to take into account that both redox properties and acidity are supposed to intervene in the NH_3 -SCR reaction. The redox properties are suggested to control the reactivity at low temperature, while acidity is expected to play a role in the SCR reaction at high temperature [59].

In a previous work, $WO_3/Ce_xZr_{1-x}O_2$ materials were evaluated with this aim [23]. A remarkable increase of the global DeNO_x efficiency were obtained involving a NSR (Pt/Ba/Al₂O₃) + SCR ($WO_3/Ce_xZr_{1-x}O_2$) configuration because the *in situ* produced ammonia on the NSR catalyst can thereafter reacts with un-stored NO_x on the SCR catalyst. However, the NH_3 reactivity on the SCR material strongly depends on its formulation and the temperature. Indeed, SCR and SCO reactions, as well as ammonia slip, compete together. For instance, at 300°C, although the $WO_3/Ce_{0.2}Zr_{0.8}O_2$ sample presented the higher DeNO_x efficiency in coupled system, an ammonia slip of about 10% was still observed, whereas the $WO_3/Ce_{0.4}Zr_{0.6}O_2$ catalyst released

only 3 % of the *in situ* produced NH₃. Then, it clearly appears that WO₃-based oxides SCR catalyst formulation can be improved to combine both a high SCR reactivity and a low NH₃ slip for a coupled NSR+SCR system. Taking into account these results and the literature data reported above, modified alumina were prepared and evaluated in this study. Acidic and redox properties were expected by incorporation of metal ions such as cerium (for oxygen mobility), zirconium, titanium, and silica (acidic behavior). Particularly, a high degree of protonic acidity (Brønsted acid sites) is reported for mixed alumina–silica materials compared with the single oxides [60]. Moreover, the isomorphous substitution of Al³⁺ by Si⁴⁺ in tetrahedral lattice position alters the tetrahedrally coordinated Al³⁺ versus octahedral coordinated Al³⁺ ratio of the material and affects the coordinative unsaturated sites (CUS). WO₃ was selected as active phase for the NH₃-SCR reaction because of its acidic and redox behaviors. The chosen WO₃ loading (9%) was based on previous works using ceria-zirconia supports [23]. Indeed, on Ce_xZr_{1-x}O₂ supports, the optimum loading for the NH₃-SCR reaction was found between 8.6 and 10 % [61,62]. In this work, all the prepared samples were evaluated in NH₃-SCR reaction before and after WO₃ impregnation. In addition to textural measurements, the more interesting samples were also characterized in terms of acidic and redox properties as well as for the selective catalytic oxidation of ammonia (NH₃-SCO). Finally, their association downstream a Pt/Ba/Al₂O₃ catalyst in a NSR+SCR coupled process was examined, with a special attention to the use of the *in situ* produced ammonia.

1. EXPERIMENTAL PART

1.1. Catalysts preparation

The mixed oxides for SCR experiments were synthesized using the sol-gel method based on the protocol developed by Pinnavaia *et al.* [63,64,65].

First, the P123 triblock copolymer was dissolved in butanol at 36°C. Then, the aluminum precursor (aluminum sec-butoxide), and if any, the silicium one (TetraEthyl Ortho Silicate - TEOS), is added at 15°C under continuous stirring. After one hour, titania isopropoxide (diluted in butanol) and/or cerium nitrate (diluted in water) and/or zirconium oxinitrate (diluted in water) were added in order to obtain final molar ratio of 1.0 Al³⁺ : 0.2 P123 : 15.5 butanol : 3.75 H₂O. After stirring for 4h, the obtained gel is matured for 40 h at 60°C in an autoclave. The resulting gel is filtered and washed with butanol, and finally calcined at 600 °C under dry air (heating rate: 1°C min⁻¹).

The resulting material are named $A_aB_bC_cD_d$ where the capital letters correspond to the element and the subscript ones indicate the atomic ratio.

On these supports, 9 wt% WO_3 were added by impregnation of the corresponding amount of ammonium metatungstate. This addition was carried out at 60°C under continuous agitation. After drying at 80°C, the resulting powder was placed in an oven for a night. Finally, the solid was calcined under wet air (10 % H_2O) during 4 h at 700°C.

A 1%Pt-10%BaO/ Al_2O_3 catalyst ($161\text{ m}^2\text{g}^{-1}$) was used as NSR model catalyst. Preparation method and main characteristics are depicted in a previous work [23]. First, barium was deposited on the alumina powder by precipitation of barium salt ($Ba(NO_3)_2$) and platinum was secondly impregnated with a $Pt(NH_3)_2(NO_2)_2$ aqueous solution. The catalyst was finally stabilized at 700°C for 4 h under a mixture containing 10 % O_2 , 10 % H_2O in N_2 .

1.2. Characterization technics and catalytic tests

All the characterization technics used in this study are detailed in a previous work [23]. Only the main data are reported here.

1.2.1. Textural characterizations

Nitrogen adsorption-desorption isotherms were recorded at -196°C, using a Tristar 3000 Micromeritics apparatus, after outgassing under vacuum for 8 h at 250°C.

1.1.2. Structural analysis

X-ray powder diffraction was performed at room temperature (RT) with a Bruker D5005 using a $K\alpha$ Cu radiation ($\lambda=1.54056\text{ \AA}$). The powder was deposited on a silicon monocrystal sample holder. The crystalline phases were identified by comparison with the ICDD database files.

1.2.3. NH_3 storage

The ammonia storage capacities were measured at 200, 300 and 400°C. Before analysis, the sample (60mg) was pretreated in situ for 30 min at 550°C under a 10 % O_2 , 10 % H_2O , 10% CO_2 and N_2 gas mixture. A flow containing 500 ppm NH_3 , 10 % CO_2 , 10 % H_2O and N_2 (total flow rate: 12 L h^{-1}) was injected until ammonia saturation (obtained after approximately 300s). Gas concentrations were recorded with a MKS 2030 Multigas infrared analyzer. The stored quantity of ammonia was calculated taking into account the reactor volume.

1.2.4. Pyridine adsorption followed by infrared spectroscopy

The surface acidity of the materials was evaluated by pyridine adsorption monitored by IR spectroscopy (Nexus Nicolet spectrometer equipped with a DTGS detector; resolution of 4 cm^{-1}

¹ and 64 scans). The spectra were normalized to a disc of 10 mg/cm². After activation at 450°C, pyridine was adsorbed at RT and desorption was performed up to 450°C, by step of 50°C.

1.2.5. Temperature programmed reduction with hydrogen (*H₂-TPR*)

Temperature programmed reduction (TPR) experiments were performed under 1 vol.% H₂ in Ar flow, from RT up to 900°C (heating rate: 5°C min⁻¹) on a Micromeritics Autochem 2920 apparatus equipped with a TCD. The sample was firstly calcined *in situ* at 300°C for 30 min under 10 vol.% O₂ in Ar flow and purged at RT under Ar flow for 45 min.

1.2.5. Oxygen storage capacity (*OSC*)

The OSC was measured at 400°C under atmospheric pressure. The sample was continuously purged with helium. Alternate pulses of pure O₂ and pure CO were injected every 2 min [66]. The oxygen storage capacity (OSC) was calculated from the CO₂ formation during alternate pulses of CO and O₂.

1.2.7. *NH₃-SCR and NH₃-SCO catalytic tests*

The selective catalytic reduction (SCR) activity measurements were performed under a gas flow depicted in Table 1 and simulating realistic Diesel engine exhaust conditions.

In an oxidising environment (which is the case of diesel engines), several chemical reactions can occur depending on the NO/NO₂ ratio, as presented in the introduction part. As its name suggests, fast SCR (Eq. 2) is preferable. However, only NO was selected as introduced NO_x for the SCR tests since in the NSR+SCR combined system, NO₂ is assumed to be mostly stored on the NSR catalyst. Tests were carried out in a quartz tubular micro-reactor. 60 mg of SCR catalyst was used in each run, and the total flow rate was fixed at 12 L h⁻¹, corresponding to a GHSV of about 160 000 h⁻¹ (GHSV, calculated as the volume of feed gas / volume of catalyst). The compositions of the inlet and outlet gas mixtures were monitored using online MKS Multigas infrared analyzer. The N₂ selectivity was calculated assuming that no other N-compounds than NO, NO₂, N₂O and NH₃ are formed. The catalytic activity for NH₃-SCR of NO is expressed by the following equation:

$$X_{\text{NO}} (\%) = ([\text{NO}]_{\text{inlet}} - [\text{NO}]_{\text{outlet}}) / [\text{NO}]_{\text{inlet}} \times 100 \quad (\text{Eq. 5})$$

The selective catalytic oxidation (SCO) experiments were carried out using similar protocol as previously depicted for SCR test, except that NO was replaced by the same flow of N₂ (Table 1).

Table 1. Catalytic test conditions. Rich and lean gas compositions used for the NO_x conversion test in alternate cycles (60s lean / 3s rich); NH₃-SCR and NH₃-SCO gas mixtures. Lean mixture was also used for the NO_x storage measurements. Total flow rate: 12 L h⁻¹.

Catalytic tests	Gas	NH ₃	NO	H ₂	O ₂	CO ₂	H ₂ O	N ₂
NSR	Rich		-	3 %	-	10 %	10 %	Balance
	Lean		500 ppm	-	10 %	10 %	10 %	
NH ₃ -SCR		500 ppm	500 ppm	-	10 %	10 %	10 %	Balance
NH ₃ -SCO		500 ppm	-	-	10 %	10 %	10 %	Balance

1.2.8. NO_x storage reduction test (cycled conditions)

NO_x storage reduction experiments were performed using NSR catalyst alone (NSR tests, 60mg of Pt-Ba/Al + 120 mg of inert SiC), or in association with a SCR material downstream (NSR+SCR combined system, 60 mg of Pt-Ba/Al + 120 mg of SCR catalyst). Before measurements, the catalytic bed was treated *in situ* at 450°C under 3 % H₂, 10 % H₂O, 10 % CO₂ and N₂ for 15 min. The sample was then cooled down to reaction temperature (200, 300 and 400°C) under the same mixture. NO_x conversions were measured in cycling conditions by alternatively switching between lean and rich gas mixtures described in Table 1 using electrovalves. The lean and rich periods were 60s and 3s, respectively. Note that only the stored NO_x during the lean periods can be reduced using this procedure since there is no reductant in the lean mixture and no NO_x in the rich one. Most gases (NO, NO₂, N₂O, NH₃, CO, CO₂,...) were analyzed using a Multigas FTIR detector (MKS 2030), except H₂ which was analyzed by mass spectrometry. NO_x conversion is calculated using Eq.5. Results are also expressed as NH₃ yield which corresponds to the percentage of introduced NO_x which is converted into ammonia.

2. RESULTS AND DISCUSSION

2.1. Investigation on dopant effect in NH₃-SCR reaction-Formulation screening

In this first part of the study, the catalytic behavior and the textural properties of the different studied samples are summarized, starting from the simple alumina (Al) which was thereafter modified by different elements: Al-Ce, Al-Ce-Zr, Al-Ce-Ti, Al-Ce-Zr-Ti and finally Al-Si-Ce-Zr-Ti. All prepared samples were evaluated before and after WO₃ impregnation. The influence of the formulation is summarized in Table 2 where the temperatures for NO_x conversion of 20, 50 and 80% are reported, as well as BET surface area and mean pore diameters. Additional information, like light-off profiles, are supplied in the Supplementary Information (SI) file.

Table 2. Textural characterization and NOx SCR behavior of the studied formulation.

Formulation	Catalysts	S _{BET} (m ² /g)	d _{BJH} (nm)	T ₂₀ (°C)	T ₅₀ (°C)	T ₉₀ (°C)
Al	Al ₂ O ₃	442	7.2	/	/	/
	WO ₃ /Al ₂ O ₃	293	4.2	/	/	/
Al _(1-x) Ce _x	Al _{0.96} Ce _{0.04}	453	5.8			
	WO ₃ /Al _{0.96} Ce _{0.04}	260	4.2	236		
Al _(1-2x) Ce _x Zr _x	Al _{0.92} Ce _{0.04} Zr _{0.04}	319	5.2			
	WO ₃ /Al _{0.92} Ce _{0.04} Zr _{0.04}	302	4.8	313		
Al _(1-2x) Ce _x Ti _x	Al _{0.92} Ce _{0.04} Ti _{0.04}	310	5.6			
	WO ₃ /Al _{0.92} Ce _{0.04} Ti _{0.04}	281	4.8	287		
	Al _{0.84} Ce _{0.08} Ti _{0.08}	251	6.1	395		
	WO ₃ /Al _{0.84} Ce _{0.08} Ti _{0.08}	235	5.7	226	290	
	Al _{0.68} Ce _{0.16} Ti _{0.16}	175	5.4			
	WO ₃ /Al _{0.68} Ce _{0.16} Ti _{0.16}	156	5.7	214	271	
	Al _{0.52} Ce _{0.24} Ti _{0.24}	130	7.3	313		
	WO ₃ /Al _{0.52} Ce _{0.24} Ti _{0.24}	123	6.6	205	258	
	Al _{0.36} Ce _{0.32} Ti _{0.32}	105	7.6	257		
	WO ₃ /Al _{0.36} Ce _{0.32} Ti _{0.32}	89	6.9	195	246	
Al _(1-x) Ce _x Zr _x Ti _x	Al _{0.88} Ce _{0.04} Zr _{0.04} Ti _{0.04}	291	5.1			
	WO ₃ /Al _{0.88} Ce _{0.04} Zr _{0.04} Ti _{0.04}	247	4.6	270		
Al _(1-5x/2) Ce _{x/2} Zr _x Ti _x	Al _{0.80} Ce _{0.04} Zr _{0.08} Ti _{0.08}	252	4.5			
	WO ₃ /Al _{0.80} Ce _{0.04} Zr _{0.08} Ti _{0.08}	225	4.6	280		
	Al _{0.6} Ce _{0.08} Zr _{0.16} Ti _{0.16}	203	6.1	335		
	WO ₃ /Al _{0.6} Ce _{0.08} Zr _{0.16} Ti _{0.16}	191	6.6	225	284	
	Al _{0.4} Ce _{0.12} Zr _{0.24} Ti _{0.24}	163	6.5	270		
	WO ₃ /Al _{0.4} Ce _{0.12} Zr _{0.24} Ti _{0.24}	128	6.8	220	279	
	Al _{0.2} Ce _{0.16} Zr _{0.32} Ti _{0.32}	121	7.4	220	300	
WO ₃ /Al _{0.2} Ce _{0.16} Zr _{0.32} Ti _{0.32}	91	7.5	200	242	296	
Al _a Si _b Ce _c Zr _d Ti _f	Al _{0.1} Si _{0.1} Ce _{0.16} Zr _{0.32} Ti _{0.32}	169	5.7	220	260	310
	WO ₃ /Al _{0.1} Si _{0.1} Ce _{0.16} Zr _{0.32} Ti _{0.32}	125	6.4	215	260	310

Alumina, as well as $\text{WO}_3/\text{Al}_2\text{O}_3$, do not exhibit any SCR activity. Only a slight ammonia oxidation into NO_x is observed, from 300°C with alumina alone, and 350°C with $\text{WO}_3/\text{Al}_2\text{O}_3$. Cerium addition to alumina, which was reported to stabilize the alumina structure for low loading [67], allows some N_2 formation from 250°C , but it is attributed to ammonia oxidation (maximum conversion of 40 % at 500°C) and not to NO_x reduction because the NO_x outlet concentration is not significantly lowered. On the contrary, with the corresponding sample impregnated with WO_3 , the NO_x conversion starts from 150°C , but it is limited to 30% in the $250\text{-}420^\circ\text{C}$ temperature range. It thereafter decreases due to ammonia oxidation by O_2 . In fact, ammonia is fully converted from 420°C .

Based on these previous results, $\text{Al}_2\text{O}_3\text{-CeO}_2$ based formulation was completed by addition of Zr ($\text{Al}_{0.92}\text{Ce}_{0.04}\text{Zr}_{0.04}$) or Ti ($\text{Al}_{(1-2x)}\text{Ce}_x\text{Ti}_x$ with $0.04 \leq x \leq 0.4$).

Firstly, Zr incorporation in $\text{Al}_{0.92}\text{Ce}_{0.04}\text{Zr}_{0.04}$ leads mainly to a limitation of the ammonia oxidation, but still without De NO_x activity. For the WO_3 containing samples, it also leads to a decrease in the De NO_x efficiency at low temperature. The temperature for 20% NO_x reduction (T20) increases from 236°C for $\text{WO}_3/\text{Al}_{0.96}\text{Ce}_{0.04}$ to 313°C with Zr incorporation ($\text{WO}_3/\text{Al}_{0.92}\text{Ce}_{0.04}\text{Zr}_{0.04}$) (Table 2), probably due to a lower NO_2 formation rate (standard SCR *versus* fast SCR). However, according to a limitation of the ammonia oxidation by O_2 with Zr incorporation, a better use of ammonia is observed at high temperature. The NO_x conversion increases with temperature until 40 % in the $420\text{-}500^\circ\text{C}$ temperature range (light-off profiles are reported in the SI file).

Overall, similar behaviors were observed with Ti or Zr addition in Al-Ce solid. However, a small NO_x reduction is observed with $\text{Al}_{0.92}\text{Ce}_{0.04}\text{Ti}_{0.04}$ compared with $\text{Al}_{0.92}\text{Ce}_{0.04}\text{Zr}_{0.04}$, and $\text{WO}_3/\text{Al}_{0.92}\text{Ce}_{0.04}\text{Ti}_{0.04}$ is a little more active in NO_x reduction than $\text{WO}_3/\text{Al}_{0.92}\text{Ce}_{0.04}\text{Zr}_{0.04}$, with a T20 of 287°C (Table 2). Taking into account these observations, further materials were evaluated increasing the Ce-Ti ratio, keeping an equal atomic loading for Ce and Ti.

Before WO_3 impregnation, data reported in Table 2 clearly indicate that the increase of the Ce-Ti atomic loading in $\text{Al}_{(1-2x)}\text{Ce}_x\text{Ti}_x$ ($0.04 \leq x \leq 0.4$) leads to a significant improvement of the SCR activity, with a decrease of the onset temperature. In addition to T20 and T50 reported in Table 2, the maximum NO_x conversion varies from 6 % to 65 % for $x=0.04$ and $x=0.4$, respectively. As already observed with the previously presented samples, WO_3 impregnation strongly improves the SCR activity, and a continuous decrease of T20 and T50 is observed increasing the Ce-Ti loading (Figure 1A). The maximum NO_x conversion is limited for $0.08 \leq x \leq 0.032$ at approximately 70 % (globally in the $350\text{-}400$ temperature range), and it is improved to 87 % (observed in the $300\text{-}340^\circ\text{C}$ temperature range) for $x=0.4$. In parallel, textural analysis of these

samples show a decrease of the BET surface area (Table 2), indicating that the improvement of the SCR activity is not related to the available surface, but probably to an increase of the active sites number and density. Indeed, the SCR reaction needs both acidic sites for NH₃ adsorption and redox sites for reaction. In the studied materials, both types of sites may be different and the proximity of these sites should also impact the activity. However, the maximum NO_x conversion also appears to vary with the mean pore diameter (Figure 2A). The relationship between DeNO_x efficiency and pore size diameter is not well established in the literature. Nevertheless, in a binary-oxides system, Qu *et al.* [68] have observed that an appropriate pore diameter promotes the dispersion of some amorphous oxide as well as rational ratio of Ce⁴⁺/Ce³⁺.

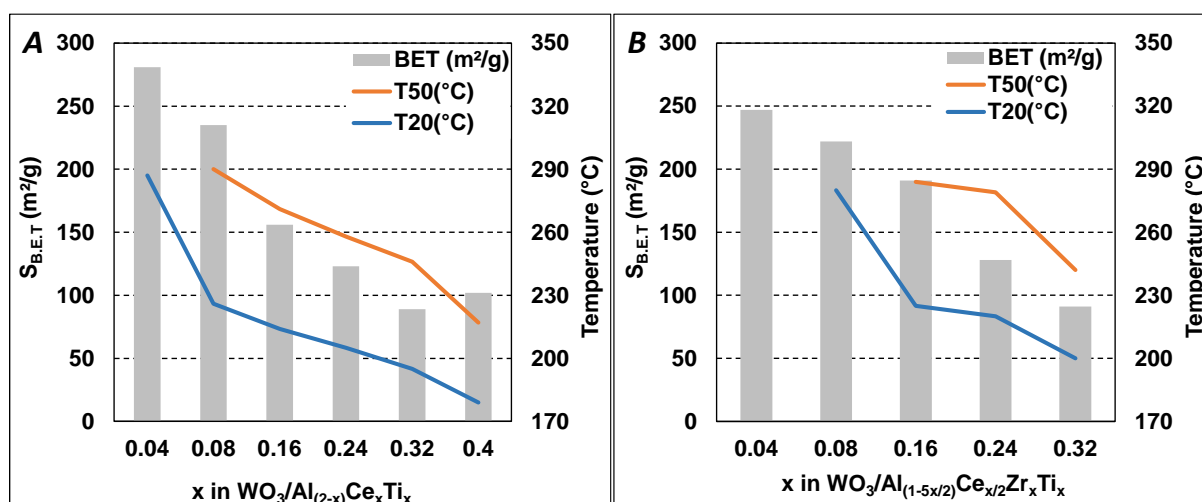


Figure 1. Specific surface area, and catalytic behaviour (temperature for 20% (T20) and 50% (T50) of NO_x conversion), depending of x atomic ratio in (A): WO₃/Al_(2-x)Ce_xTi_x and (B): WO₃/Al_(1.5x/2)Ce_{x/2}Zr_xTi_x catalysts.

Finally, the increase of the Ce-Ti loading allows a great improvement of the NO_x conversion at low temperature but, for all these samples, the NO_x conversion decreases at high temperature (from 300 to 400°C depending of the formulation) due to competition between the NH₃ + NO_x reaction (SCR) and the NH₃ + O₂ reaction (SCO). Taking into account that previously studied Zr containing sample (WO₃/Al_{0.92}Ce_{0.04}Zr_{0.04}) exhibited limited NH₃ oxidation behavior, new formulations with Ce, Zr and Ti were evaluated.

Firstly, a formulation with equal atomic ratio for the three metals was synthesized: (WO₃)/Al_{0.88}Ce_{0.04}Zr_{0.04}Ti_{0.04} (Table 2). Unfortunately, the NO_x SCR activity of this formulation remains low, even after WO₃ impregnation. The NO_x conversion reaches a maximum of 24 % at 300°C, it drops near zero in the 350-450°C temperature range, and the

outlet NO_x concentration exceeds the inlet value for higher temperatures, with detection of NO₂. Ammonia is fully converted at 500°C. In fact, this WO₃/Al_{0.88}Ce_{0.04}Zr_{0.04}Ti_{0.04} catalyst exhibits mainly oxidation behavior, even better than WO₃/Al_{0.92}Ce_{0.04}Ti_{0.04} and WO₃/Al_{0.92}Ce_{0.04}Zr_{0.04}. No synergetic effect is observed. As Ce is supposed to be the main contributor for the oxidation properties, new solids were prepared with a two times lower relative cerium loading, respecting the formulation (WO₃)/Al_(1-5x/2)Ce_{x/2}Zr_xTi_x with 0.04 ≤ x ≤ 0.32.

Before WO₃ addition, the catalytic activity is very low for x=0.04 and 0.08, as for the NO_x reduction (maximal NO_x conversion of 6 %), as for ammonia conversion (20% at 500°C). The DeNO_x efficiency gradually increases for 0.16 ≤ x ≤ 0.32, with maximum NO_x conversions between 24 % and 57 % around 400°C. For higher temperatures, the ammonia conversion still increases, but it never reaches 100 % at 500°C (maximum of 80 % for Al_{0.2}Ce_{0.16}Zr_{0.32}Ti_{0.32}). Compared with Al_(1-2x)Ce_xTi_x formulations, these materials exhibit lower oxidation behavior, which is also put in evidence in regard of NO₂ outlet concentration at 500°C: 35 ppm were recorded at 500°C for Al_{0.2}Ce_{0.16}Zr_{0.32}Ti_{0.32}, whereas 85 ppm NO₂ were detected for Al_{0.2}Ce_{0.4}Ti_{0.4}.

Again, WO₃ addition leads to a large enhancement of the DeNO_x efficiency. Temperatures for 20 % and 50 % of NO_x conversion decrease with x in WO₃/Al_(1-5x/2)Ce_{x/2}Zr_xTi_x, from 280°C to 200°C for T20, and from 284 to 242°C for T50. Note that half NO_x conversion is not reached for x=0.08. These data are specifically reported in Figure 1B, as the continuous decrease of the specific surface areas with x, from 247 to 91 m²g⁻¹, indicating again that the catalytic activity improvement is attributable to an increase of the active sites number with x, but not to the specific surface area. In addition, the maximum NO_x conversion also increase with x. It is limited at 26 % for x=0.08 and reaches 85 % for x=0.32, globally in the 350-400°C temperature range (Figure 2B). In fact, it appears in this figure that this maximum NO_x conversion also varies with the mean pore diameter of the sample, as previously observed with WO₃/Al_(1-2x)Ce_xTi_x samples.

Finally, WO₃/Al_{0.2}Ce_{0.16}Zr_{0.32}Ti_{0.32} exhibits a high NO_x conversion (85 %) in a relatively large temperature range (350-425°C). Moreover, the ammonia oxidation at high temperature is rather limited and ammonia tends to be fully converted only at 500°C, compared to 450°C for WO₃/Al_{0.2}Ce_{0.4}Ti_{0.4}. Comparison of these two samples shows that the NO_x concentration exhibits only a small increase at high temperature for WO₃/Al_{0.2}Ce_{0.16}Zr_{0.32}Ti_{0.32} (+ 50 ppm between the lower NO_x value and the concentration at 500°C) whereas a difference of 150 ppm is observed with WO₃/Al_{0.2}Ce_{0.4}Ti_{0.4}. As a conclusion, ammonia appears less reactive over Al-Ce-Zr-Ti samples than over Al-Ce-Ti materials.

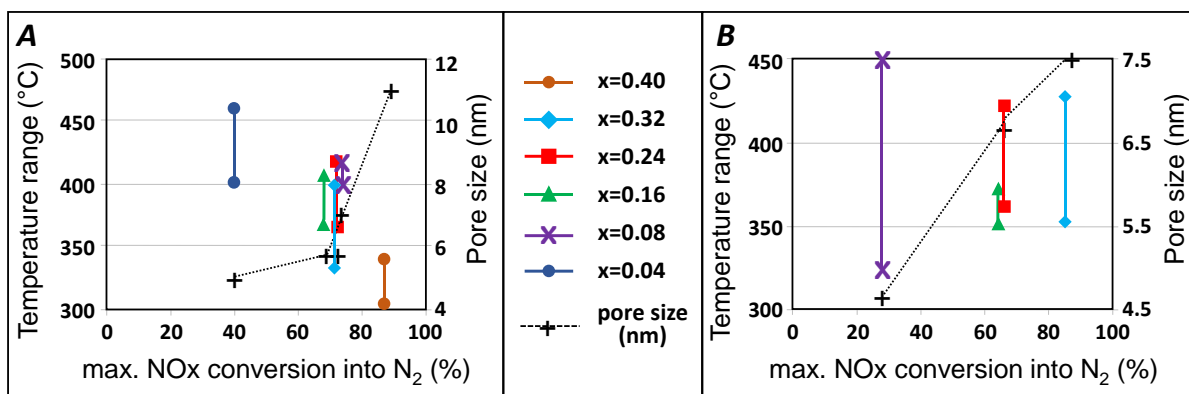


Figure 2. Relation between the maximum NO_x conversion (and its temperature range) and the mean pore diameter of (A): $\text{WO}_3/\text{Al}_{(1-2x)}\text{Ce}_x\text{Ti}_x$ and (B) $\text{WO}_3/\text{Al}_{(1-5x/2)}\text{Ce}_{x/2}\text{Zr}_x\text{Ti}_x$ catalysts.

With the aim to improve the ammonia reactivity without enhancement of the redox behavior to prevent the reactivity toward oxygen, a supplementary element, Si, was introduced in the more interesting Al-Ce-Zr-Ti composition, respecting the following formulation: $(\text{WO}_3)/\text{Al}_{0.1}\text{Si}_{0.1}\text{Ce}_{0.16}\text{Zr}_{0.32}\text{Ti}_{0.32}$. Silica addition was expected to increase the acidity of the solid. The resulting solids exhibit specific surface areas of 169 and 125 m^2g^{-1} before and after WO_3 impregnation, respectively (Table 2).

Interestingly, results reported in Table 2 indicates that this formulation is highly active in NO_x reduction, even before WO_3 addition. Indeed, both NO_x conversions curves are close until 80% NO_x conversion. However, tungsten addition allows a higher maximal NO_x conversion, at 88% in the 350-390°C temperature range, versus 83 % in the 330-350°C temperature range without WO_3 . Unfortunately, for both formulations, NO_x conversion is significantly deteriorated at high temperature. At 500°C, it reaches only 50 and 60 % for $\text{Al}_{0.1}\text{Si}_{0.1}\text{Ce}_{0.16}\text{Zr}_{0.32}\text{Ti}_{0.32}$ and $\text{WO}_3/\text{Al}_{0.1}\text{Si}_{0.1}\text{Ce}_{0.16}\text{Zr}_{0.32}\text{Ti}_{0.32}$, respectively.

Considering all the studied samples, in addition to the SCR activity at low temperature, it appears that the maximum NO_x conversion strongly varies with the formulation. It generally depends on the reactivity of ammonia at high temperature, with the competition between the reaction with NO_x or its oxidation, probably by O₂ (into N₂ or NO_x, both leading to a lack of ammonia to reduce NO_x).

Taking into accounts these results, three formulations exhibiting the more interesting SCR behaviors were selected for further characterizations and catalytic test in a NSR+SCR coupled process: $\text{WO}_3/\text{Al}_{0.2}\text{Ce}_{0.4}\text{Ti}_{0.4}$, $\text{WO}_3/\text{Al}_{0.2}\text{Ce}_{0.16}\text{Zr}_{0.32}\text{Ti}_{0.32}$ and $\text{WO}_3/\text{Al}_{0.1}\text{Si}_{0.1}\text{Ce}_{0.16}\text{Zr}_{0.32}\text{Ti}_{0.32}$. Their respective T₅₀ are 217, 242 and 260°C, and no N₂O was detected during the SCR tests. The full NO_x concentration profiles versus temperature are available in Figure 4B.

2.2. Characterization of the selected catalysts

In this part, the three selected materials ($\text{WO}_3/\text{Al}_{0.2}\text{Ce}_{0.4}\text{Ti}_{0.4}$, $\text{WO}_3/\text{Al}_{0.2}\text{Ce}_{0.16}\text{Zr}_{0.32}\text{Ti}_{0.32}$ and $\text{WO}_3/\text{Al}_{0.1}\text{Si}_{0.1}\text{Ce}_{0.16}\text{Zr}_{0.32}\text{Ti}_{0.32}$) were characterized by means of XRD analysis, NH_3 storage capacity, pyridine adsorption, H_2 -TPR, OSC and NH_3 -SCO experiments.

2.2.1. XRD analysis

XRD patterns of three selected samples are reported in the supplementary file (Figure SI.1). Solids appear rather amorphous, which was expected taking into account the material composition and the obtained specific surface areas. More precisely, only CeO_2 oxide is detected in $\text{WO}_3/\text{Al}_{0.2}\text{Ce}_{0.4}\text{Ti}_{0.4}$, and only ZrO_2 is detected in $\text{WO}_3/\text{Al}_{0.2}\text{Ce}_{0.16}\text{Zr}_{0.32}\text{Ti}_{0.32}$. The particle sizes deduced from the Scherrer equation are approximately 4.5 nm and 7.5 nm, respectively. Diffraction peaks are broader for the $\text{WO}_3/\text{Al}_{0.1}\text{Si}_{0.1}\text{Ce}_{0.16}\text{Zr}_{0.32}\text{Ti}_{0.32}$ sample, probably indicating the presence of Ce and/or Zr oxides. No particle size is reasonably calculable. Finally, no relationship between the DeNO_x activity and the catalyst structure can be easily established.

2.2.2. Acidic properties

Acidic properties were characterized by both ammonia storage capacity measurements (200, 300, 400°C) and pyridine adsorption monitored by FTIR.

As expected, the ammonia storage capacity decreased with increasing temperature (Table 3), showing that the strength of the acidic sites of the studied supports appears rather weak. The NH_3 storage amounts are very close for $\text{WO}_3/\text{Al}_{0.2}\text{Ce}_{0.4}\text{Ti}_{0.4}$ and $\text{WO}_3/\text{Al}_{0.2}\text{Ce}_{0.16}\text{Zr}_{0.32}\text{Ti}_{0.32}$, demonstrating that Zr incorporation do not enhance amount or strength of acidic sites. To the opposite, Si addition leads to a significant improvement of the amount of acidic sites. The increase is about 40% compared with the other formulations, whatever the temperature.

Nevertheless, these ammonia storage capacity measurements in dynamic condition do not allow to determine the nature of acidic sites (i.e. Lewis or Brønsted). To the opposite, pyridine adsorption monitored by FTIR is a powerful technique largely used to characterize the surface acidity of solids [69]. The IR spectra of samples obtained after pyridine adsorption at RT and evacuation at 150°C are depicted in Figure 3A for the frequency range of ring ν_{CCN} vibration (1650-1400 cm^{-1}).

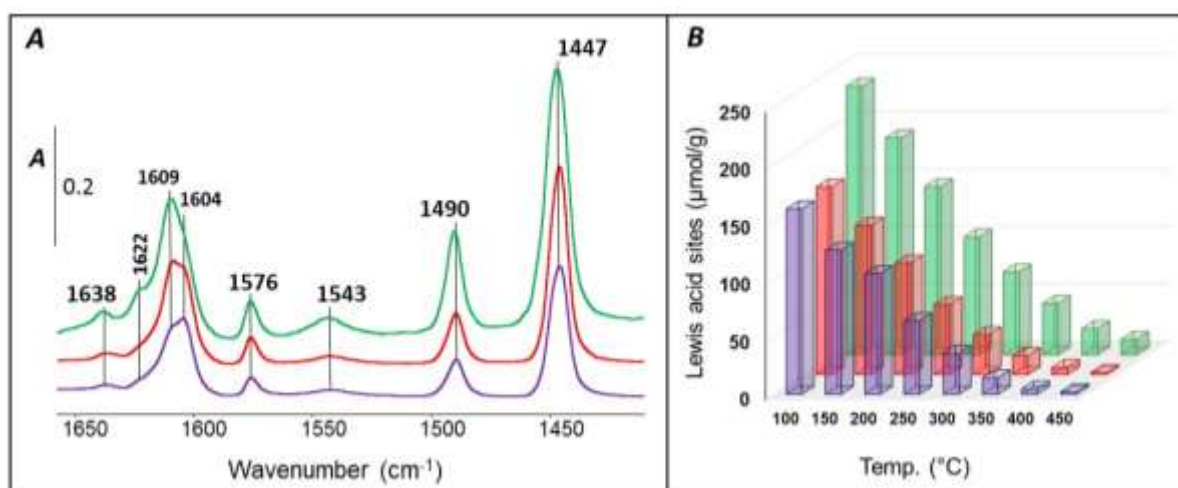


Figure 3. Infrared spectra of pyridine adsorbed at room temperature followed by evacuation at 150°C (A) and Lewis acid sites ($\mu\text{mol/g}$) amount (B). (— $\text{WO}_3/\text{Al}_{0.2}\text{Ce}_{0.4}\text{Ti}_{0.4}$; — $\text{WO}_3/\text{Al}_{0.2}\text{Ce}_{0.16}\text{Zr}_{0.32}\text{Ti}_{0.32}$ and — $\text{WO}_3/\text{Al}_{0.1}\text{Si}_{0.1}\text{Ce}_{0.16}\text{Zr}_{0.32}\text{Ti}_{0.32}$ catalysts).

Characteristic frequencies of pyridine coordinated to Lewis acid sites (LAS) were observed at 1447 cm^{-1} (ν_{19b}), 1490 cm^{-1} (ν_{19a}), 1576 cm^{-1} (ν_{8b}) and at $1604\text{--}1622\text{ cm}^{-1}$ (ν_{8a}). The position and the multiplicity of the ν_{8a} ring vibration of chemisorbed pyridine on Lewis acid sites is related to their nature, their number and their strength. Thus, the occurrence of the ν_{8a} mode of ν_{CCN} vibrations at three different frequencies (1604 , 1609 and 1622 cm^{-1}) on alumina-based oxides indicates the presence of heterogeneous Lewis acid sites having different strengths.

According to Zaki *et al.* [70], the ν_{8a} band at 1604 cm^{-1} is assigned to pyridine coordination on Ti^{4+} . The band at 1609 cm^{-1} is consistent with previous work which denotes ν_{8a} -absorption at 1610 cm^{-1} over tungstated ceria-zirconia samples [23], whereas the ν_{8a} band at 1622 cm^{-1} is suggested to be assigned to pyridine coordinated to tetrahedral Al^{3+} (strong LAS) [71]. Note that the amount of strong LAS (ν_{8a} at 1622 cm^{-1}) is enhanced in $\text{WO}_3/\text{Al}_{0.1}\text{Si}_{0.1}\text{Ce}_{0.16}\text{Zr}_{0.32}\text{Ti}_{0.32}$ catalyst. In addition, formation of pyridinium surface species is observed in all samples, characterized by ν_{8a} -absorption at 1638 cm^{-1} in association to ν_{19b} -absorption mode at 1543 cm^{-1} .

Table 3. H₂-TPR and OSC experiments of WO₃ supported catalysts.

Catalyst	H ₂ -TPR			total H ₂ cons. (μmol/g)	OSC CO ₂ formed (μmol/g)	NH ₃ -storage (μmol/g)		
	T peak(s)	(°C)				200°C	300°C	400°C
WO ₃ /Al _{0.2} Ce _{0.4} Ti _{0.4}	/	726	830 ^{sh}	1129	8	90	24	14
WO ₃ /Al _{0.2} Ce _{0.16} Zr _{0.32} Ti _{0.32}	/	715	/	543	7	94	24	13
WO ₃ /Al _{0.1} Si _{0.1} Ce _{0.16} Zr _{0.32} Ti _{0.32}	503 ^w	683		392	1	130	34	18

w: weak ; sh: shoulder

To conclude, in addition to ammonia storage experiments, the acidic characterization by FTIR reveals that both Lewis and Brønsted acid sites are present over all the studied catalysts. Silica-containing support develops higher amount of Brønsted acid sites that was assigned to the formation of Si-OH-Al linkages of silanol groups located in close vicinity to an Al atom in tetrahedral environment, as in amorphous silica alumina for instance [72]. The proportion of Brønsted acid sites of WO₃/Al_{0.1}Si_{0.1}Ce_{0.16}Zr_{0.32}Ti_{0.32} catalysts is about 10% of the total number of acidic sites, against only 5% for Si-free samples. As reported in Figure 3B, the strength and the number of Lewis acid sites is also enhanced with the Si content. WO₃/Al_{0.1}Si_{0.1}Ce_{0.16}Zr_{0.32}Ti_{0.32} exhibits acid sites strong enough to retain pyridine up to 450°C. Interestingly, in accordance with NH₃ storage capacities, the evolution of LAS in function of the temperature of pyridine evacuation (Figure 3B) is similar for WO₃/Al_{0.2}Ce_{0.4}Ti_{0.4} and WO₃/Al_{0.2}Ce_{0.16}Zr_{0.32}Ti_{0.32} catalysts.

2.2.3 Redox properties

Redox properties were firstly evaluated in terms of reducibility by hydrogen using TPR experiments (Table 3). WO₃-supported catalysts exhibits a mean reduction peak in the 683-726°C temperature range, depending on the material composition. It corresponds to the easily reducible Ce^{IV} reduction into Ce^{III}. WO₃/Al_{0.2}Ce_{0.4}Ti_{0.4} catalyst, which presents the higher Ce loading (x=0.4), also exhibits the higher H₂ consumption (Table 3) compared to WO₃/Al_{0.2}Ce_{0.16}Zr_{0.32}Ti_{0.32} and WO₃/Al_{0.1}Si_{0.1}Ce_{0.16}Zr_{0.32}Ti_{0.32} samples (x=0.16).

Note that for the WO₃ free host supports, the reduction peak is observed in a lower temperature range (630-705°C). In addition, the total the H₂ consumption is higher compared with the WO₃ containing catalysts, and depends on the catalysts formulation. The H₂ consumption is approximately 7 %, 30 % and 60 % higher for Al_{0.2}Ce_{0.4}Ti_{0.4}, Al_{0.2}Ce_{0.16}Zr_{0.32}Ti_{0.32} and

$\text{Al}_{0,1}\text{Si}_{0,1}\text{Ce}_{0,16}\text{Zr}_{0,32}\text{Ti}_{0,32}$ supports, respectively. Taking into account that only Ce^{IV} is supposed to be reducible, this observation clearly highlights that WO_3 -Ce interactions strongly depend on the support formulation. It appears that the more the catalyst is acidic, the more the inhibiting effect of WO_3 on the sample reducibility is strong.

Secondly, redox properties were evaluated in terms of oxygen storage capacity (OSC) measured at 400°C . Results concerning the CO oxidation into CO_2 are reported in Table 3. The CO_2 formation over WO_3 -supported catalysts is ranked between $1 \mu\text{mol g}^{-1}$ to $8 \mu\text{mol g}^{-1}$ depending on the support formulation. In absence of tungsten oxide, the OSC is significantly higher. $\text{Al}_{0,2}\text{Ce}_{0,4}\text{Ti}_{0,4}$ and $\text{Al}_{0,2}\text{Ce}_{0,16}\text{Zr}_{0,32}\text{Ti}_{0,32}$ supports exhibit close OSC values, with $29 \mu\text{mol CO}_2 \text{ g}^{-1}$ and $33 \mu\text{mol CO}_2 \text{ g}^{-1}$, respectively. $\text{Al}_{0,1}\text{Si}_{0,1}\text{Ce}_{0,16}\text{Zr}_{0,32}\text{Ti}_{0,32}$ presents the lower OSC value, with $11 \mu\text{mol g}^{-1}$. These results are in accordance with those obtained from the TPR experiments: the largest loss of redox properties of WO_3 -supported catalysts is denoted for $\text{Al}_{0,1}\text{Si}_{0,1}\text{Ce}_{0,16}\text{Zr}_{0,32}\text{Ti}_{0,32}$ support, supporting again the impact of the support acidity on the tungsten-cerium interaction.

2.2.4. NH_3 -SCO

Results of NH_3 oxidation by O_2 are presented in Figure 4A (gas composition reported in Table 1). To highlight these behaviors, corresponding NH_3 -SCR experiments are also depicted in Figure 4B for the three selected materials. It is worth noting that N_2O was not detected during these NH_3 -SCO experiments. Moreover, the ammonia oxidation is nearly fully selective into N_2 since NO_x (in fact NO) formation reached maxima of only 10-30 ppm at 500°C (dotted line Figure 4A). All the three materials start to oxidize ammonia at approximately 250°C , but SCO activities strongly vary at higher temperatures. The more complex formulation ($\text{WO}_3/\text{Al}_{0,1}\text{Si}_{0,1}\text{Ce}_{0,16}\text{Zr}_{0,32}\text{Ti}_{0,32}$) appears the more active one with a T_{80} of 368°C , whereas $\text{WO}_3/\text{Al}_{0,2}\text{Ce}_{0,4}\text{Ti}_{0,4}$, exhibits a maximal ammonia conversion of only 40 % at 500°C . These results are in accordance with the NH_3 -SCR conversions reported in Figure 4B which evidence a competition between NH_3 -SCR and NH_3 -SCO in the 350 - 500°C temperature range (previously discussed in section 2.1.). Indeed, the catalyst which presents the higher NH_3 -SCO efficiency also features of the higher ammonia oxidation in NH_3 -SCR experiments. In addition, this catalysts exhibits the higher acidic behaviors and the higher W-Ce interactions.

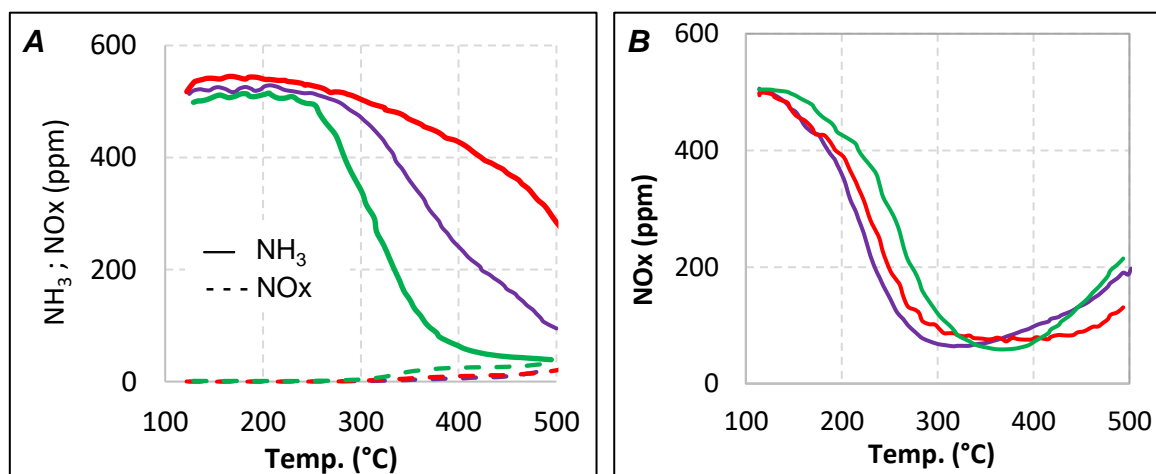


Figure 4. NH₃-SCO (A) and NH₃-SCR (B) versus temperature for $\text{WO}_3/\text{Al}_{0.2}\text{Ce}_{0.4}\text{Ti}_{0.4}$; $\text{WO}_3/\text{Al}_{0.2}\text{Ce}_{0.16}\text{Zr}_{0.32}\text{Ti}_{0.32}$ and $\text{WO}_3/\text{Al}_{0.1}\text{Si}_{0.1}\text{Ce}_{0.16}\text{Zr}_{0.32}\text{Ti}_{0.32}$ catalysts.

2.3. NSR + SCR combination system

NO_x reduction efficiency was studied in dual NSR+SCR catalytic bed (60 mg of Pt-Ba/Al + 120 mg of SCR catalyst, downstream) in order to increase the global NO_x conversion. More precisely, the aim was to use the *in situ* produced NH₃ over the NSR catalyst during the rich pulses of the NSR cycles. NO_x reduction in cycled condition was performed at 200, 300, 400°C by switching for 3 s in rich media every 63 s (lean phase), as reported in Table 1. Both NO_x conversion and ammonia yield (percentage of introduced NO_x which is converted into ammonia) are illustrated in Figure 5, as well as N-compounds profiles recorded during NSR cycles (300°C).

Firstly, for single Pt-Ba/Al, it was previously established that whatever the tested temperature, the NO_x conversion is always lower than the NO_x storage rate for 60s in NSR process [23]. Then, the reduction step is the limiting step of the cycled process. Maximum NO_x conversion is reached at 300°C (64 %, dotted line in Figure 5A₂). In the same time, the introduced hydrogen during the rich pulses is not fully converted (H₂ conversion reaches only between 36 % and 82 % between 200°C and 400°C, respectively). As previously reported in [73], it favors NH₃ emission. It was clearly putted in evidence an ammonia intermediate pathway for the reduction of the stored NO_x with H₂. For the single Pt-BaAl catalyst, ammonia yield is then ranking between 10 % and 35 % (dotted line, Figure 5B₂).

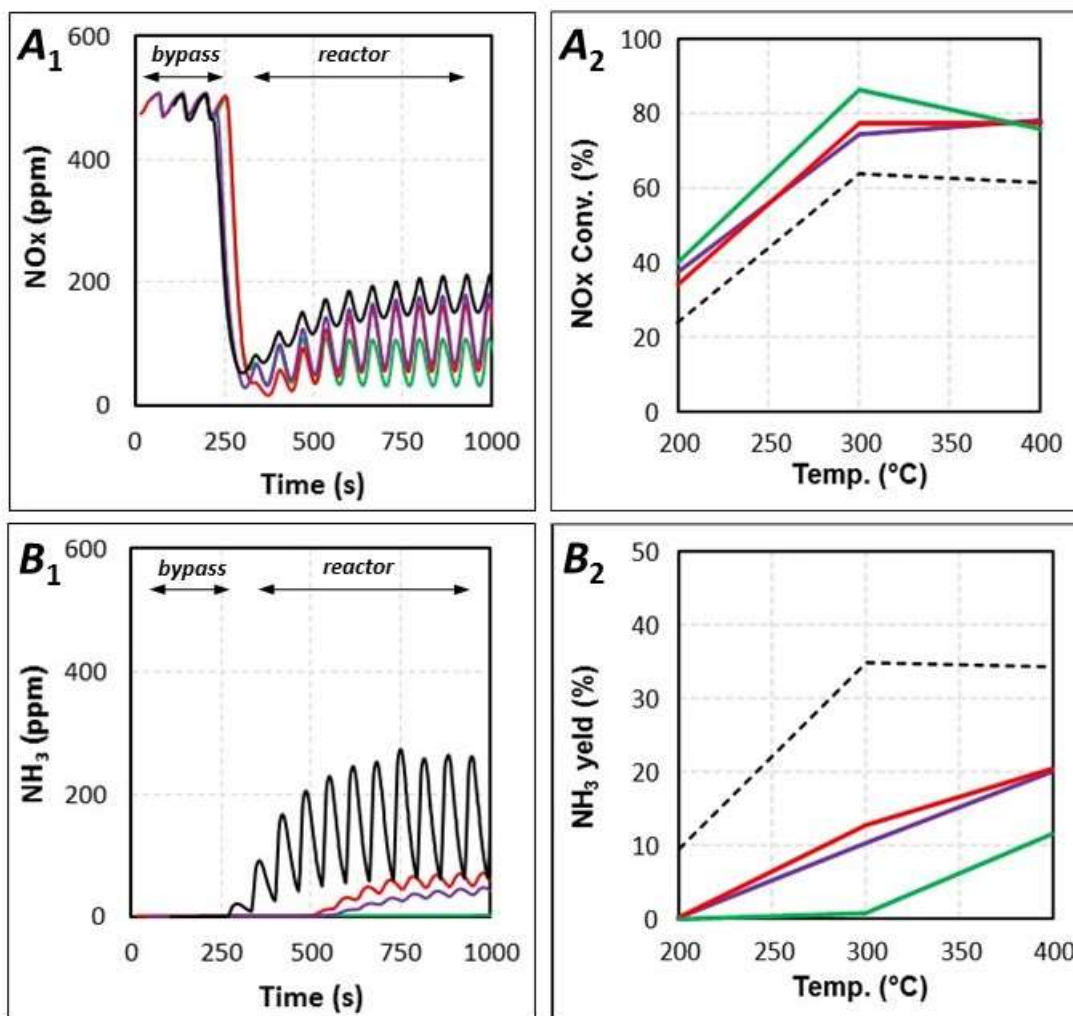


Figure 5. Effect of the combination downstream of the SCR catalytic materials in the double bed (NSR + SCR) on NO_x (A1) and NH₃ (B1) outlet profiles for NSR cycles experiments at 300°C; NO_x conversion (A2) and NH₃ yield (B2) versus temperature. (---, Pt-BaAl+SiC; ---, Pt-BaAl+WO₃/Al_{0.2}Ce_{0.4}Ti_{0.4}; ---, Pt-BaAl+WO₃/Al_{0.2}Ce_{0.16}Zr_{0.32}Ti_{0.32} and --- Pt-BaAl+WO₃/Al_{0.1}Si_{0.1}Ce_{0.16}Zr_{0.32}Ti_{0.32} catalyts).

For the NSR + SCR coupled system, Figure 5A₂ shows that, whatever the SCR formulation, the DeNO_x efficiency is significantly enhanced. The maximum NO_x conversion (86 %) is obtained at 300°C with WO₃/Al_{0.1}Si_{0.1}Ce_{0.16}Zr_{0.32}Ti_{0.32} placed downstream the Pt-BaAl sample, also illustrated by the NO_x profiles reported in Figure 5A₁. In the same time, the ammonia yield is remarkably decreased. In fact, Figure 5B indicated that the NSR+SCR system is fully selective into N₂ at 200°C whatever the SCR catalyst formulation. For higher temperatures (*i.e.* 300°C and 400°C), ammonia emission still occur, but in a lower extent. In addition, the ammonia release is delayed when the SCR catalyst is placed downstream of the NSR material, as depicted Figure 5B1 for tests at 300°C. It indicates that ammonia is fully stored during the first cycles for WO₃/Al_{0.2}Ce_{0.4}Ti_{0.4} and WO₃/Al_{0.2}Ce_{0.16}Zr_{0.32}Ti_{0.32}. With WO₃/Al_{0.1}Si_{0.1}Ce_{0.16}Zr_{0.32}Ti_{0.32}, which is the more acidic material, ammonia is fully stored and

converted at 300°C even after stabilization. Note that no significant supplementary H₂ consumption was observed with the implementation of the SCR samples downstream, indicating that the enhancement in NO_x conversion is only correlated to the ammonia conversion. In addition, no N₂O was observed during these tests in cycling condition.

Therefore, the ammonia consumption after addition of a SCR catalyst directly reflects the activity of SCR materials in the double bed association. More precisely, taking into account the gas composition after the NSR catalyst alone, and after the NSR+SCR coupled system, it is possible to evaluate the use of NH₃ on the downstream SCR catalyst.

The amount of NH₃ emitted from the single NSR catalyst is reported in Figure 6A (in gray) and corresponds to 48, 174 and 171 ppm at 200, 300 and 400°C, respectively. The use of the *in situ* produced ammonia on the SCR catalysts was determined taking into accounts three possibilities: the NH₃-SCR reaction (NH₃+NO_x→N₂), the NH₃-SCO reaction (NH₃+O₂→N₂) and the unconverted NH₃. The ammonia converted by the NH₃-SCR reaction was calculated considering that each additional converted NO_x is associated with one converted NH₃. Supplementary ammonia conversion is associated with the SCO reaction, considering a fully selective reaction into N₂, as demonstrated in section 2.2.4. Thus, the use of ammonia by the SCR catalyst is reported Figure 6, considering the three previously mentioned reactions (NH₃-SCR, NH₃-SCO and NH₃ released).

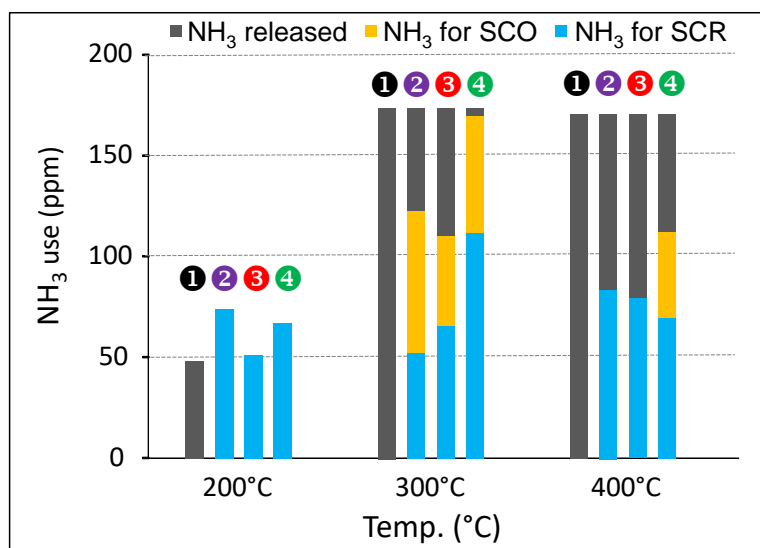


Figure 6. NH₃ use (ppm) in NSR+SCR coupled system (①— Pt-BaAl+SiC; ②— Pt-BaAl+WO₃/Al_{0.2}Ce_{0.4}Ti_{0.4}; ③— Pt-BaAl+WO₃/Al_{0.2}Ce_{0.16}Zr_{0.32}Ti_{0.32} and ④— Pt-BaAl+WO₃/Al_{0.1}Si_{0.1}Ce_{0.16}Zr_{0.32}Ti_{0.32} catalysts).

As previously illustrated in Figure 5B₂, only the NH₃-SCR reaction occurs at 200°C whatever the considered SCR catalyst. The additional converted NO_x are even higher than the amount of the available ammonia emitted from the single NSR catalyst, especially for WO₃/Al_{0.2}Ce_{0.4}Ti_{0.4} (#2 on Figure 6) and WO₃/Al_{0.1}Si_{0.1}Ce_{0.16}Zr_{0.32}Ti_{0.32} (#3 on Figure 6) catalysts. This supplementary NH₃ production at 200°C can be explained by the formation of isocyanate species during the mixture of the rich and lean fronts where NO, CO₂ and H₂ were present together. Water (10 % vol.) rapidly hydrolyzed these species and supplementary ammonia can be formed and then reduce supplementary NO_x [74] at 200°C.

On the opposite, the three pathways (NH₃-SCR, NH₃-SCO and unconverted NH₃) take place at 300 and 400°C, with proportions depending on the SCR catalyst formulation (Figure 6). At 300°C, WO₃/Al_{0.1}Si_{0.1}Ce_{0.16}Zr_{0.32}Ti_{0.32} exhibits both the lower NH₃ release (4 ppm) and the higher ammonia consumption in NH₃-SCR (112 ppm). The two samples without silica (WO₃/Al_{0.2}Ce_{0.4}Ti_{0.4} and WO₃/Al_{0.2}Ce_{0.16}Zr_{0.32}Ti_{0.32}) present significantly higher unconverted NH₃, with 51 ppm and 63 ppm, respectively. However, it seems that Zr incorporation enhances the NH₃-SCR activity, since 53 ppm and 67 ppm NH₃ are converted for this reaction over WO₃/Al_{0.2}Ce_{0.4}Ti_{0.4} and WO₃/Al_{0.2}Ce_{0.16}Zr_{0.32}Ti_{0.32}, respectively.

At 400°C the oxidation of NH₃ by O₂ (NH₃-SCO) is not observed on WO₃/Al_{0.2}Ce_{0.4}Ti_{0.4} and WO₃/Al_{0.2}Ce_{0.16}Zr_{0.32}Ti_{0.32} catalysts. WO₃/Al_{0.1}Si_{0.1}Ce_{0.16}Zr_{0.32}Ti_{0.32} is still the sample which presents the lower amount of unconverted NH₃, but the NH₃-SCO reaction represents an ammonia consumption of about 42 ppm on this sample.

In the coupled system, the aim is to use the available reductant to increase the global DeNO_x efficiency and to prevent ammonia slip. Ammonia released is then a major concern. The catalytic behavior of Si-containing solid developed in this study is thereafter compared to results obtained in a previous work with WO₃/Ce-Zr samples [23]. More precisely, the distribution of the use of the *in situ* produced ammonia, i.e. the reaction with NO_x (NH₃-SCR), O₂ (NH₃-SCO) or unreacted NH₃, is depicted in Figure 7. Note that the increasing of the DeNO_x efficiency in the coupled system (NSR+SCR) is assumed to be directly correlated to the portion of ammonia used in the NH₃-SCR pathway. At 200°C (not shown), NH₃ always reacts exclusively with NO_x, whatever the catalyst composition. The higher NO_x conversion is reached with WO₃/Al_{0.1}Si_{0.1}Ce_{0.16}Zr_{0.32}Ti_{0.32} catalysts. For higher temperature, as mentioned above, the three pathways compete. The WO₃/Ce-Zr (20-80) and WO₃/Al_{0.1}Si_{0.1}Ce_{0.16}Zr_{0.32}Ti_{0.32} materials reach close behaviour in NH₃-SCR. At 300°C (Figure 7A), the Si-containing solid and WO₃/Ce-Zr (20-80) release very low amount of ammonia, but WO₃/Al_{0.1}Si_{0.1}Ce_{0.16}Zr_{0.32}Ti_{0.32} catalyst exhibits a better SCR/SCO ratio than WO₃/Ce-Zr (20-

80). Same trend is observed at 400°C (Figure 7B), even if the ammonia release becomes higher for the Si-containing solid compare with WO₃/Ce-Zr (20-80). WO₃/Al_{0.1}Si_{0.1}Ce_{0.16}Zr_{0.32}Ti_{0.32} is then an interesting solution to enhance the global DeNO_x efficiency, even if it could be improved with enhancement in strong acidic sites number.

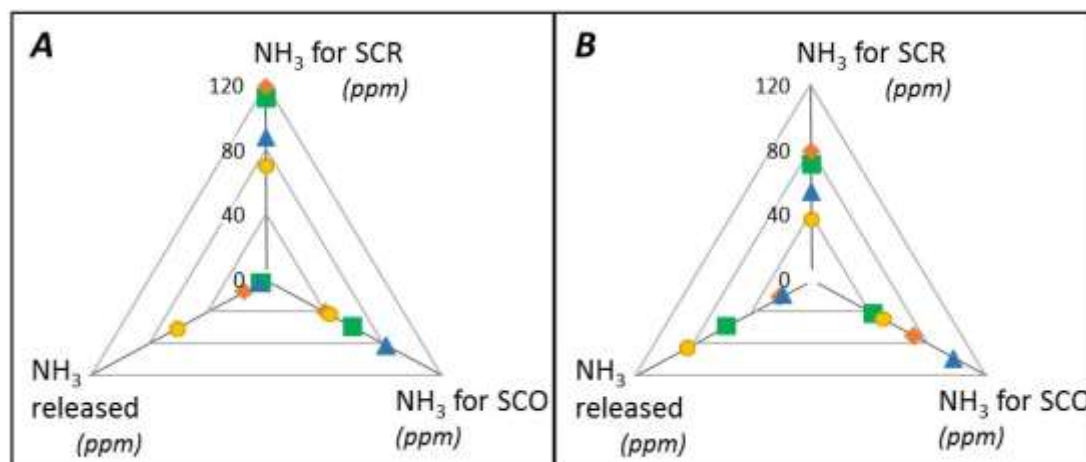


Figure 7. Comparative behaviours of ammonia used (ppm) in NH₃-SCR, NH₃-SCO and NH₃ released for tungstated catalysts in NSR +SCR coupled system at (A): 300°C and (B): 400°C. (■): WO₃/Al_{0.1}Si_{0.1}Ce_{0.16}Zr_{0.32}Ti_{0.32}; (◆): WO₃/Ce-Zr (20-80); (▲): WO₃/Ce-Zr (40-60); (●): WO₃/Ce-Zr (70-30).

3. CONCLUSION

With the aim to develop active NH₃-SCR materials for the specific NSR+SCR coupled system, alumina-mixed oxides were synthesized by sol-gel route. The incorporation of active supposed dopant (Ce, Zr, Ti, Si) was investigated and the activity of catalysts was determined in NH₃-SCR before and after WO₃ impregnation. The atomic loading ratio of added dopants ($0.04 \leq x \leq 0.4$) was investigated. Among the thirty prepared materials, three formulations present promising NH₃-SCR behaviors, namely WO₃/Al_{0.2}Ce_{0.4}Ti_{0.4}, WO₃/Al_{0.2}Ce_{0.16}Zr_{0.32}Ti_{0.32} and WO₃/Al_{0.1}Si_{0.1}Ce_{0.16}Zr_{0.32}Ti_{0.32} catalysts. Acidic properties is enhanced by Si incorporation, which is assumed to favor WO₃ – Ce interaction, leading to a significant loss of the redox properties. The three selected WO₃-supported catalysts are active in NO_x reduction by NH₃, and fully selective in N₂. These solids can reduce 50 % of NO_x compounds at 217, 242 or 260°C for WO₃/Al_{0.2}Ce_{0.4}Ti_{0.4}, WO₃/Al_{0.2}Ce_{0.16}Zr_{0.32}Ti_{0.32} and WO₃/Al_{0.1}Si_{0.1}Ce_{0.16}Zr_{0.32}Ti_{0.32}, respectively, including CO₂ and H₂O in feed gas.

Placed downstream a Pt-Ba/Al model NSR catalyst, results showed an increase of the global NO_x conversion in all cases and all temperatures, together with a strong decrease of released

NH₃. However, from 300°C, NH₃-SCR and NH₃-SCO compete. Interestingly, at 400°C, WO₃/Al_{0.2}Ce_{0.4}Ti_{0.4} and WO₃/Al_{0.2}Ce_{0.16}Zr_{0.32}Ti_{0.32} catalysts are fully selective towards NH₃+NO_x reaction pathways. At this temperature, the reaction competition of NH₃ with NO_x or O₂ is only present over WO₃/Al_{0.1}Si_{0.1}Ce_{0.16}Zr_{0.32}Ti_{0.32}. Nevertheless, this solids exhibits the lower NH₃ slip, with virtually no ammonia emitted at 300°C at the reactor outlet. Combined with exceptionally increased NO_x conversion rate, this formulation offers interesting behaviors even if it could be improved again with enhancement in strong acidic sites number.

REFERENCES:

- [1] T. Kobayashi, T. Yamada, K. Kayano, SAE Technical Papers 970745 (1997) 63.
- [2] L. Masdrag, X. Courtois, F. Can, D. Duprez, Appl. Catal. B. 146 (2014) 12-23
- [3] I. Nova, L. Lietti, L. Castoldi, E. Tronconi and P. Forzatti, J. Catal. 239 (2006), 244–254.
- [4] Z. Liu and J.A. Anderson, J. Catal. 224 (2004) 18-27.
- [5] H. Abdulhamid, E. Fridell, M. Skoglundh, Top. Catal. 30/31 (2004) 161-168.
- [6] L. Castoldi, I. Nova, L. Lietti, P. Forzatti, Catal. Today 96 (2004) 43-52.
- [7] I. Nova, L. Castoldi, L. Lietti, E. Tronconi, P. Forzatti, Catal. Today 75 (2002) 431–437.
- [8] I. Nova, L. Lietti, P. Forzatti, Catal. Today 136 (2008) 128-135.
- [9] N. Le Phuc, X. Courtois, F. Can, S. Berland, S. Royer, P. Marecot, D. Duprez, Catal. Today 176 (2011) 424-428.
- [10] N. Le Phuc, X. Courtois, F. Can, S. Royer, P. Marecot, D. Duprez, Appl. Catal. B 102 (2011) 353–361.
- [11] M. Konsolakis, I.V. Yentekakis, J. Catal. 198 (2001) 142-150.
- [12] J. Shibata, K.I. Shimizu, A. Satsuma, T. Hattori, Appl. Catal. B. 37 (2002) 197-204.
- [13] E.F. Iliopoulou, A.P. Evdou, A.A. Lemonidou, I.A. Vasalos, Appl. Catal. A. 274 (2004) 179-189.
- [14] K. Arve, F. Klingstedt, K. Eränen, J. Wärnä, L.E. Lindfors, D. Yu. Murzin, Chem. Eng. J. 107 (2005) 215-220.
- [15] I. Sobczak, M. Ziolk, M. Nowacka, Micropor. Mesopor. Mat. 78 (2005) 103-116.
- [16] S.C. Chen, S. Kawi, Appl. Catal. B. 45 (2003) 63-76.
- [17] L.F. Cordoba, W.M.H. Sachtler, C.M. De Correa, Appl. Catal. B. 56 (2005) 269-277.
- [18] I.V. Yentekakis, V. Tellou, G. Botzolaki, I.A. Rapakousios, Appl. Catal. B.56 (2005) 229-239.
- [19] T. Maunula, J. Ahola, H. Hamada, Appl. Catal. B. 26 (2000) 173-192.
- [20] M.Koebel,; M. Elsener, O. Kröcher, C. Schär, R. Röthlisberger, F. Jaussi, M. Mangold, Topics Catal. 30/31 (2004) 43-48.
- [21] L. Xu, R.W. McCabe, R.H. Hammerle, Appl. Catal. B. 39 (2002) 51-63.
- [22] J.A. Sullivan, J.A. Doherty, Appl. Catal. B. 55 (2005) 185-194.
- [23] F. Can, S. Berland, S. Royer, X. Courtois, D. Duprez, ACS Catal. 3 (2013) 1120-1132.
- [24] M. Koebel, M. Elsener, M. Kleemann, Catal. Today 59 (2000) 335-345.
- [25] A. Väliheikki, K.C. Petallidou, C.M. Kalamaras, T. Kolli, M. Huuhtanen, T. Maunula, R.L. Keiski, A.M. Efstathiou, Appl. Catal. B 156–157 (2014) 72–83
- [26] A. Flura, F. Can, X. Courtois, S. Royer, D. Duprez, Appl. Catal B 126(2012) 275-289.
- [27] F. Can, A. Flura, X. Courtois, S. Royer, G. Blanchard, P. Marecot, D. Duprez, Catal. Today 164 (2011) 474-479.
- [28] L. Lietti, I. Nova, P. Forzatti, J. Catal. 257 (2008) 270-282.

-
- [29] M. Koebel, G. Madia, M. Elsener, *Catal. Today* 73 (2002) 239-247.
- [30] I. Nova, C. Ciardelli, E. Tronconi, D. Chatterjee, B. Bandl-Konrad, *Catal. Today* 114 (2006) 3-12.
- [31] P. Forzatti, L. Lietti, E. Tronconi, in: I.T. Horvath (Ed.), *Nitrogen Oxides Removal—Industrial. Encyclopaedia of Catalysis*, first ed., Wiley, New York, 2002, and references therein
- [32] A. Kato, S. Matsuda, T. Kamo, F. Nakajima, H. Kuroda, T. Narita, *J. Phys. Chem.* 85 (1981) 4099-4102.
- [33] H. Bosch, F. Janssen, *Catal. Today* 2 (1988) 369-532.
- [34] J. Due-Hansen, S.B. Rasmussen, E. Mikolajska, M.A. Banares, P. Ávila, R.Fehrmann, *Appl. Catal. B* 107 (2011) 340-346.
- [35] M. Casanova, E. Rocchini, A. Trovarelli, K. Scherzanz, I. Begsteiger, *J. Alloys Compd.* 408–412 (2006) 1108-1112.
- [36] M. Casanova, K. Scherzanz, J Llorca, A. Trovarelli, *Catal. Today* 184 (2012) 227-236.
- [37] A. Shi, X. Wang, T. Yu, M. Shen, *Appl. Catal. B* 106 (2011) 359-369.
- [40] G. Blanchard, S. Rousseau L. Mazri, L. Lizarraga, A. Giroir-Fendler, B. D’Anna, P. Vernoux, *European Patent* 11708906.0-2113 (2011)
- [41] J. H. Park, H. J. Park, J. H. Baik, I. S. Nam, C. H. Shin, J. H. Lee, B. K. Cho, S. H. Oh, *J. Catal.* 240 (2006) 47-57.
- [42] J. A. Sullivan, O. Keane, *Appl. Catal. B* 61 (2005) 244-252.
- [43] K. Krishna, G.B.F. Seijger, C.M. Van den Bleek, H.P.A. Calis, *Chem. Commun.* (2002) 2030-2031.
- [44] R.Q. Long, R.T Yang, *J. Catal.* 188 (1999) 332-339.
- [45] A.Z. Ma, W. Grunert, *Chem. Commun.* (1999) 71-72.
- [46] G. Carja, G. Delahay, C. Signorile, B. Coq, *Chem. Commun.* (2004) 1404-1405.
- [47] S. Brandenberger, O. Kröcher, A. Tissler, R. Althoff, *Catal. Rev.* 50 (2008) 492-531.
- [48] J. Li, H. Chang, L. Ma, J. Hao, R.T. Yang, *Catal. Today* 175 (2011) 147-156.
- [49] M. Koebel, M. Elsener, G. Madia, *Ind. Eng. Chem. Res.* 40 (2001) 52-59.
- [50] M. Koebel, G. Madia, M. Elsener, *Catal. Today* 73 (2002) 239-247.
- [51] Y. Yeom, J. Henao, M. Li, W.M.H. Sachtler, E. Weitz, *J. Catal.* 231 (2005) 181-193.
- [52] C. Ciardella, I. Nova, E. Tronconi, D. Chatterjee, T. Burkhardt, M. Weibel, *Chem. Eng. Sci.* 62 (2007) 5001-5006.
- [53] N. Apostolescu, B. Geiger, K. Hizbullah, M.T. Jan, S. Kureti, D. Reichert, F. Schott, W. Weisweiler, *Appl. Catal. B.* 62 (2006) 104-114.
- [54] G.S. Qi, R.T. Yang, R. Chang, *Appl. Catal. B* 51 (2004) 93-106.
- [55] L.Chen, J.Li, M. Ge, R. Zhu, *Catal. Today* 153 (2010) 77–83.
- [56] W. Shan, F. Liu, H. He, X. Shi, C. Zhang, *Appl. Catal. B* 115-116 (2012) 100-106.
- [57] W. Shan, F. Liu, H. He, X. Shi, C. Zhang, *Chem. Commun.* 47 (2011) 8046-8048.
- [58] J.P. Chen, R.T. Yang, *Appl. Catal. A* 80 (1992) 135-148.
- [59] L. Lietti, *Appl. Catal. B.* 10 (1996) 281-297.
- [60] W Daniell, U Schubert, R Glöckler, A Meyer, K Noweck, H Knözinger, *Appl. Catal. A* 196 (2000) 247-260
- [61] Y. Li, H. Cheng, Y. Qin, Y. Xie, S. Wang, *Chem. Commun.* (2008) 1470-1472.
- [62] X. W. Li, M. M. Shen, H. Xi, H. Y. Zhu, F. Gao, K. Yan, D. Lin and C. Yi, *J. Phys. Chem. B* 109 (2005) 3949-3955.
- [63] S. A. Bagshaw, E. Prouzet, T. J. Pinnavaia, *Science* 269 (1995) 1242-1244.
- [64] S. A. Bagshaw, T. J. Pinnavaia, *Angew. Chem., Int. Ed. Engl.* 35 (1996) 1102-1105.
- [65] W. Zhang, T. J. Pinnavaia, *Chem. Commun.* (1998) 1185-1186.
- [66] S. Kacimi, J. Jr. Barbier, R. Taha, D. Duprez, *Catal. Lett.* 22 (1993) 343-350.
- [67] W. Zhang, T. J. Pinnavaia, *Chem. Commun.* (1998) 1185-1186.

-
- [68] L. Qu, C. Li, G. Zeng, M. Zhang, M. Fu, J. Ma, F. Zhan, D. Luo, *Chem. Eng. J.* 242 (2014) 76-85
- [69] E.P. Parry, *J. Catal.* 2 (1963) 371-379.
- [70] M.I. Zaki, M.A. Hasan, F.A. Al-Sagheer, L. Pasupulety, *Colloids and Surfaces A.* 190 (2001) 261-274.
- [71] C. Morterra, G. Magnacca, *Catal. Today* 27 (1996) 497-532.
- [72] G. Crepeau, V. Montouillou, A. Vimont, L. Mariey, T. Cseri, F. Mauge, *J. Phys.Chem. B* 110 (2006) 15172–15185.
- [73] N. Le Phuc, X. Courtois, F. Can, S. Royer, P. Marecot, D. Duprez, *Appl. Catal. B.* 102 (2011) 362-371.
- [74] E.C. Corbos, M. Haneda, X. Courtois, P. Marecot, D. Duprez, H. Hamada, *Catal. Comm.* 10 (2008) 137-141.